Gargantuan Hail in Argentina

Matthew R. Kumjian* and Rachel Gutierrez

Department of Meteorology and Atmospheric Science, The Pennsylvania State University, University Park, Pennsylvania, USA

Joshua S. Soderholm

Meteorological Institute, University of Bonn, Germany

Stephen W. Nesbitt

Department of Atmospheric Sciences, University of Illinois at Urbana-Champaign, Urbana, Illinois, USA

Paula Maldonado

Centro de Investigaciones del Mar y la Atmósfera/CONICET-UBA, Departamento de Ciencias de la Atmósfera y los Océanos/FCEN- UBA, UMI-IFAECI 3355/ CNRS-CONICET-UBA, Buenos Aires, Argentina

Lorena Medina Luna

National Center for Atmospheric Research, Boulder, Colorado, USA

James Marquis

Pacific Northwest National Laboratory, Richland, Washington, USA

Early Online Release: This preliminary version has been accepted for publication in *Bulletin of the American Meteorological Society*, may be fully cited, and has been assigned DOI 10.1175/BAMS-D-19-0012.1. The final typeset copyedited article will replace the EOR at the above DOI when it is published.

Kevin A. Bowley

Department of Meteorology and Atmospheric Science, The Pennsylvania State University, University Park, Pennsylvania

Milagros Alvarez Imaz and Paola Salio

Centro de Investigaciones del Mar y la Atmósfera/CONICET-UBA, Departamento de Ciencias de la Atmósfera y los Océanos/FCEN-UBA, UMI-IFAECI 3355/ CNRS-CONICET-UBA, Buenos Aires, Argentina

*Corresponding author address: Department of Meteorology and Atmospheric Science, The Pennsylvania State University, University Park, Pennsylvania

E-mail: kumjian@psu.edu

Accepted for publication in *Bulletin of the American Meteorological Society*. DOI 10.1175/BAMS-D-19-0012.1.

ABSTRACT

Accepted for publication in *Bulletin of the American Meteorological Society*. DOI 10.1175/BAMS-D-19-0012.1.

On 8 February 2018, a supercell storm produced gargantuan ($>$ 15 cm or $>$ 6 inches in maximum dimension) hail as it moved over the heavily populated city of Villa Carlos Paz in Córdoba Province, Argentina, South America. Observations of gargantuan hail are quite rare, but the large population density here yielded numerous witnesses and social media pictures and videos from this event that document multiple large hailstones. The storm was also sampled by the newly installed operational polarimetric C-band radar in Córdoba. During the RELAMPAGO campaign, the authors interviewed local residents about their accounts of the storm, and uncovered additional social media video and photographs revealing extremely large hail at multiple locations in town. This article documents the case, including the meteorological conditions supporting the storm (with the aid of a high-resolution WRF simulation), the storm's observed radar signatures, and three noteworthy hailstones observed by residents. These hailstones include a freezer-preserved 4.48-inch (11.38$-$cm) maximum dimension stone that was scanned with a 3D infrared laser scanner, a 7.1-inch (18-cm) maximum dimension stone, and a hailstone photogrammetrically estimated to be between 7.4 and 9.3 inches (18.8 $-$ 23.7-cm) in maximum dimension, which is close to or exceeds the world record for maximum dimension. Such a well-observed case is an important step forward in understanding environments and storms that produce gargantuan hail, and ultimately how to anticipate and detect such extreme events. (Capsule Summary) Gargantuan hail fell in Argentina on 8 February 2018, including one hailstone that is possibly a world-record for maximum dimension. We document eyewitness and social media accounts of the hail, and analyze the parent storm and its environment.

Accepted for publication in *Bulletin of the American Meteorological Society*. DOI 10.1175/BAMS-D-19-0012.1.

1. Introduction

Hail can cause significant damage to property and agriculture, as well as injuries or even deaths; in part, the risk associated with hail increases with increasing hailstone size, which generally leads to greater impact kinetic energy. The current definitions for hail size based on the National Weather Service include "sub-severe," "severe," and "significantly severe" (Table 1). In the scientific literature, some studies have also identified "giant" hail as those stones with maximum dimensions exceeding 10 cm. In the taxonomy of hail sizes listed in Table 1, we also propose a new size class for hailstones with maximum dimensions exceeding 15 cm or 6 inches (referred to here as "gargantuan hail") to represent the upper extreme of hail sizes. Owing to the rarity of such extreme events, however, only a few studies have specifically documented giant or gargantuan hail events (e.g., Knight and Knight 2005; Blair and Leighton 2012; Pojorlie et al. 2013; Witt et al. 2018), and most are individual case studies rather than multi-case comparisons. Knight and Knight (2005) described the physical characteristics of giant and gargantuan hailstones from the Aurora, Nebraska storm of 2003. Every stone they studied exhibited an outer (i.e., final) growth layer indicating wet growth, and in some cases this layer was of quite substantial thickness. This implies that the hailstones went through heavy wet growth in their last moments in the updraft, just above the in-storm 0 °C level. They suggested that an extremely strong updraft in the lower portion of the hail growth zone is required to produce such large hail. Blair and Leighton (2012) used social media reports to survey a more extensive sample of giant hail reports than was present in the *Storm Data* database alone, yielding hailstones that ultimately became certified state records. They suggest that the occurrence of giant or gargantuan hail is significantly underreported. Using crowdsourced photographs and videos from a tornadic supercell in El Reno, Oklahoma, Seimon et al. (2016) claim

Accepted for publication in *Bulletin of the American Meteorological Society*. DOI 10.1175/BAMS-D-19-0012.1.

a storm chaser video captured a hailstone that may have been > 20 cm in maximum diameter; however, there was no further discussion or analysis.

None of the aforementioned studies of giant or gargantuan hail focused on observed storm properties or environments. In contrast, Pojorlie et al. (2013) documented the synoptic and mesoscale environment of the supercell that produced the Vivian, SD, hailstone (which registers as the world record for maximum dimension: 20 cm or 8 inches), and analyzed some of the storm's radar characteristics. Their evaluation of the environment indicated that it was indeed supportive of severe convective storms, but it was not obviously supportive of such large hail as was observed. Other studies focused on radar observations of storms producing giant or gargantuan hail. Blair et al. (2011) compared equivalent radar reflectivity factor at horizontal polarization (Z_H) and radial velocity (v_r) signatures in giant-hail-producing storms to those in storms producing smaller hail. They found that giant hail was virtually always associated with supercells ($> 99\%$ of cases), and that the best discriminators of hail sizes were strong midlevel azimuthal shear in v_r associated with the mesocyclone and large values of storm-top divergence. Witt et al. (2018) performed an analysis of the 2013 El Reno, OK, storm using crowdsourced observations (see Seimon et al. 2016), WSR-88D radar data, and measurements from a mobile, polarimetric X-band radar. They focused on the fallout locations of hail > 7 cm in maximum dimension and associated dual-polarization radar signatures, finding that large hailstones (including several ≥ 15 cm in maximum dimension) often fell outside the low-level maximum Z_H. Some of this hail occurred in regions of $Z_H < 50$ dBz, but within $\sim$10 km of the updraft, consistent with findings by Kumjian et al. (2010) and Picca and Ryzhkov (2012). Additionally, Jiang et al. (2019) performed electromagnetic scattering calculations for real hailstone shapes that suggest giant- and gargantuan-sized hail may have similar dual-polarization radar characteristics to hail of smaller sizes, complicating radar-based hail detection of such large hail.

Accepted for publication in *Bulletin of the American Meteorological Society*. DOI 10.1175/BAMS-D-19-0012.1.

To synthesize the findings from these prior studies, the available evidence suggests that gargantuan-hail-producing storms typically would be supercells that form in environments that do not stand out among those associated with more "typical" supercells producing smaller hail. The radar signatures of storms with gargantuan or giant hail often are not particularly noteworthy, either, except perhaps stronger mesocyclonic rotation and divergence aloft. This implies that features commonly used by operational meteorologists to forecast and monitor severe storms may only be subtly different for extreme-hail-producing storms, making anticipation and warning for such storms a substantial challenge. Hailstone fallout locations are beneath the supecell's main updraft, and the hailstone physical characteristics themselves suggest that the hailstones undergo significant wet growth in their final growth stage within the updraft. The fact that supercells most often occur in the relatively sparsely populated U.S. Great Plains, coupled with the likely sparse concentrations of extremely large hail within individual storms, suggests that gargantuan hail may be more common than is reported (albeit still rare compared to smaller hail sizes). Thus, documentation of such extreme events is important, as discussed by Knight and Knight (2001), and a necessary first step towards understanding how such hail is produced, ultimately unlocking clues toward improved prediction and detection of such events.

Herein, we document a case from 8 February 2018 that, unlike the other cases described above, featured gargantuan hail in a populated urban region. This includes a hailstone estimated photogrammetrically to be very close to or exceeding the Vivian hailstone world record for maximum dimension. The storm occurred in Villa Carlos Paz, in the Córdoba Province of Argentina (Fig. 1), making it the first well-documented case of gargantuan hail outside the U.S. Great Plains, and the first in the Southern Hemisphere. This region is known to be prone to hail (e.g., Torre et al. 2011; Mezher et al. 2012; Cecil and Blankenship 2012; Bruick et al. 2019), though hail of giant or gargantuan size has until now not been documented there. Although the authors were

Accepted for publication in *Bulletin of the American Meteorological Society*. DOI 10.1175/BAMS-D-19-0012.1.

aware of this storm based on social media reports, this study is the result of post-storm forensic meteorological research made possible by the Remote sensing of Electrification, Lightning, And Mesoscale/microscale Processes with Adaptive Ground Observations (RELAMPAGO; Nesbitt et al., in preparation) field campaign, which also happened to be based in Villa Carlos Paz from 1 November through 15 December 2018.

The remainder of this paper is laid out as follows. Section 2 provides a detailed overview of the environment leading up to the Villa Carlos Paz supercell storm, with the aid of a high-resolution numerical simulation of the event. The evolution of observed radar signatures and the simulated storm are discussed in Section 3. The analysis of giant and gargantuan hail reports in Villa Carlos Paz is provided in Section 4. A discussion of the results and conclusions is provided in Section 5.

2. Description of the Environment

At 1200 UTC (9:00 am local time) on 8 February 2018, a broad upper-level trough was located off the west coast of Chile (not shown), which favors the presence of a warm, humid, conditionally unstable airmass conducive to severe convection over central Argentina. The 1200 UTC radiosonde launched at Córdoba Ingeniero Aeronáutico Ambrosio L.V. Taravella Airport (SACO; about 30 km east-northeast of Villa Carlos Paz) reveals several elevated mixed layers above a low-level nocturnal inversion (Fig. 2a), although the most unstable parcel convective available potential energy (MUCAPE) is only about 300 J kg^{-1} at this time. These broad-scale features are consistent with the composite pattern for supercells in this region shown by Mulholland et al. (2018), though their composite also indicates a northerly low-level jet parallel to the Sierras de Córdoba, which was absent at this time (the observed 1200 UTC SACO sounding shows only weak winds in the lower troposphere). Unsurprisingly, such environmental factors that promote

Accepted for publication in *Bulletin of the American Meteorological Society*. DOI 10.1175/BAMS-D-19-0012.1.

hailstorms in the U.S. have also been identified as important in Argentina (e.g., Mezher et al. 2012; Bruick et al. 2019).

To further examine the storm environment, we ran a doubly-nested 3-1 km grid spacing Weather Research and Forecasting (WRF; Skamarock et al. 2008) v4.1 model simulation using boundary conditions from the ERA5 fifth generation atmospheric reanalysis (Copernicus Climate Change Service 2019). The ERA5 is an hourly reanalysis dataset with 0.25° horizontal resolution and 37 vertical layers from 1000 to 1 hPa. Here, the simulation primarily is used to downscale the reanalysis boundary conditions with better-resolved topography and to examine the storm and the rapidly evolving environment leading up to it. The WRF simulation outer domain, covering much of subtropical South America, was initialized at 00 UTC 8 February and run for 24 hours; the inner 1-km nest covered central Argentina, Chile, and the adjacent Pacific Ocean, and was initialized at 18 UTC. The WRF simulation had 80 vertical levels and used the Thompson microphysics scheme (Thompson et al. 2004).

The WRF-simulated thermodynamic profiles and hodographs at 1200 and 2000 UTC at Villa Carlos Paz are shown in Fig. 2, for comparison with the 1200 UTC observed sounding at SACO. The thermodynamic and kinematic profiles at Villa Carlos Paz and SACO at 1200 UTC are qualitatively similar, with minimal MUCAPE ($\sim$300 J kg^{-1}), although a weaker capping inversion than observed) and a hodograph indicating small values (-47 m^2 s^{-2}) of 0-3-km storm-relative helicity (SRH). However, the simulation indicates an evolution toward an environment more conducive to supercells at Villa Carlos Paz during the subsequent 8-hour period. Instability increases through the development of a deep mixed layer, while the boundary layer moistened and a mid-level cap in the 625-500-hPa layer eroded. MUCAPE increased to 2241 J kg^{-1} at 2000 UTC, while most unstable convective inhibition (MUCIN) decreased in magnitude to just -10.4 J kg^{-1}. Hodograph length increased over time in response to the approaching upper-level trough, indicating an

Accepted for publication in *Bulletin of the American Meteorological Society*. DOI 10.1175/BAMS-D-19-0012.1.

increase in deep-layer vertical wind shear that is known to be supportive of supercell hailstorms (e.g., Marwitz 1972; Browning 1977; Nelson 1983; Foote 1984) and favorable for hail production owing to the resultant increase in updraft breadth (Dennis and Kumjian 2017). The $0-6$-km bulk wind difference is $\sim$20.1 m s^{-1} (39.0 kts); however, an additional $\sim$5 m s^{-1} (10 kts) of shear is found between 6 and 9 km that can contribute to storm organization (e.g., Warren et al. 2017). Further, hodograph curvature increases during this time. Assuming the Bunkers et al. (2000) left-moving supercell storm motion (shown with the red star in Figs. 2b-d), 0-3 km SRH increased in magnitude from -47 m^2 s^{-2} to -126 m^2 s^{-2}. Especially rapid changes in the simulated environment occur from 1930-2100 UTC, in part a result of upslope flow along the east side of the Sierras de Córdoba. This anabatic flow transports high-CAPE ($>$ 3000 J kg^{-1}) air up the eastern slopes of the Sierras de Córdoba over a $\sim$1-hr period prior to the storm arriving in Villa Carlos Paz (Fig. 3). As in Mulholland et al. (2019), the upslope flow also helps erode the MUCIN, and enhances low-level flow, leading to a corridor of enhanced $0-3$-km SRH values, as shown in Fig. 4. Small environmental low-level shear ($<$ 5 m s^{-1} over the lowest 2 km AGL), however, suggests weak organization of the low-level mesocyclone of any supercellular convection that would develop (e.g., Markowski and Richardson 2014; Coffer and Parker 2017), resulting in a primarily severe hail and wind threat for this event. In summary, the simulation shows the rapid mesoscale development of storm parameters favorable for supercells along the eastern terrain slope, and that the environment is not well-represented by the individual operational 1200 UTC sounding collected at SACO.

3. Overview of the Villa Carlos Paz Supercell Storm

Although there is significant radar beam blockage due to Córdoba's tall buildings and the Sierras Chicas mountains between the radar and Villa Carlos Paz, the storm's salient radar characteristics are still evident in low-level ($<2^\circ$ elevation angle) scans (Fig. 5) as observed with the operational

Accepted for publication in *Bulletin of the American Meteorological Society*. DOI 10.1175/BAMS-D-19-0012.1.

C-band radar in Córdoba (RMA1). Throughout the analysis period (1819 to 2058 UTC), the storm displayed supercellular structure. At the beginning of the analysis period (1819 UTC; not shown), two distinct cells are evident, each with separate and strong updrafts, as indicated by differential reflectivity ($Z_{\rm DR}$) columns (e.g., Kumjian et al. 2014, and references therein) aloft. The cells separate further over the next 30 minutes (Fig. 5), with the left-moving cell being favored because of the orientation of the hodograph curvature (cf. Fig. 2d). By 1850 UTC, the left-moving storm starts to acquire a hook-echo-like appendage (Markowski 2002, and references therein), and continues to organize and advance northeastward over the next 15-20 minutes. By 1926:58 UTC, the heavy precipitation core is passing south and east of Villa Carlos Paz, and a well-defined hook echo is approaching the city. The main updraft moves directly over Villa Carlos Paz, as confirmed by the pronounced bounded weak echo region (BWER; see, for example, Browning and Donaldson 1964; Marwitz 1972; Browning and Foote 1976, among many others) aloft in Z_H (Fig. 6a). Figure 6b shows that the inner edge of the BWER is marked by a $Z_{\rm DR}$ column, typical of polarimetric radar signatures in supercell storms (Kumjian and Ryzhkov 2008). Further, the inner edge of the BWER exhibits a pronounced reduction in co-polar correlation coefficient $\rho_{\rm hv}$ (Fig. 6c), which has been attributed to the presence of severe hail undergoing wet growth (Kumjian and Ryzhkov 2008; Kumjian 2013a). Similarly low $\rho_{\rm hv}$ values (< 0.5) have been observed at C band in previous cases of significantly severe hail (Picca and Ryzhkov 2012) and are consistent with scattering calculations for significantly severe hailstones (e.g., Jiang et al. 2019). Further, evidence of a polarimetric three-body scattering signature (Hubbert and Bringi 2000; Picca and Ryzhkov 2012; Kumjian 2013b, 2018) aloft at this time in $Z_{\rm DR}$ and ρ_{hv} confirms the presence of hail; though, it gives no indication of its size (e.g., Zrnić et al. 2010; Kumjian 2013b). The maximum[1] observed Z_H from any elevation angle and at any time to pass over Villa Carlos Paz

[1]The radar's absolute calibration state was unknown, so only relative values are mentioned here.

Accepted for publication in *Bulletin of the American Meteorological Society*. DOI 10.1175/BAMS-D-19-0012.1.

was nearly 12 dB lower than the storm-maximum Z_H value. Additionally, these maxima were separated by 11.8 km, indicating that the gargantuan hail did not fall in the heaviest precipitation core of the storm, but rather beneath the updraft, consistent with the conceptual model of Browning and Foote (1976) and observations by Kumjian et al. (2010), Picca and Ryzhkov (2012), and Witt et al. (2018). After 1946 UTC, the storm passed beyond Villa Carlos Paz and continued to exhibit supercellular characteristics, including a hook echo. Storm structure produced in our WRF simulation is qualitatively similar to the overall storm evolution observed with the RMA1 radar, albeit with inaccurate timing. The simulated storm displayed a long track of minimum updraft helicity (UH) approaching -700 m^2 s^{-1} (Fig. 7), demonstrating a persistent rotating updraft characteristic of supercell storms.

4. Hail Reports

There were numerous social media posts of photos and videos showing hail as it was falling, and/or retrieved after the storm. Some of these reports were featured by international news agencies. In this study, we focus on three reported instances of giant and gargantuan hail in the storm, the locations and details of which are shown in Fig. 1, and provided in Table 2.

a. Maria's Hailstone

First we describe a giant (> 10 cm) hailstone that was retrieved shortly after it fell, photographed with reference objects, and preserved in a freezer by Maria Navidad Garay (hereafter "Maria's hailstone," with its location indicated by the southernmost label in Fig. 1). Maria's hailstone is shown in Fig. 8. According to Maria, the hail fall lasted approximately 15 minutes. She experienced mainly smaller stones, and found just the one large stone in the grass. It impacted the ground with substantial force, as it had penetrated $2-3$ cm into the ground when she found it. The

Accepted for publication in *Bulletin of the American Meteorological Society*. DOI 10.1175/BAMS-D-19-0012.1.

photographs from shortly after it was retrieved (Fig. 8a,b) show a rather round stone with scalloped lobes (e.g., Knight and Knight 1970) covering much of the surface, and no large icicle lobes. This implies no preferred orientation direction in its final growth layer, presumably owing to random tumbling during its descent. She recounted that many of the stones had similar roundish shapes, with clear outsides and milky insides. During the hail fall, she recalled very little rain. After the hail, she experienced rain, but no wind. Her grass was covered with hail, including some broken pieces; she also reported accumulations of hail near her door, which were likely from runoff from the rooftop gutters. Upon surveying her property, she showed us damage to the carport roof and the hail net covering portions of her driveway. Thus, it is likely that some other large stones fell at her location, but perhaps melted, broke apart, or otherwise were not noticed. Since moving to VCP in 1986, this was by far the largest hailstone she had ever seen.

The official measurements of Maria's hailstone took place during the RELAMPAGO field campaign, after it had been preserved in her freezer for 9 months. The preserved stone had an artificially flattened base (Fig. 8c,d) from melting and refreezing in the freezer. (She was proud of her hailstone and often took it out of the freezer to show guests.) Therefore, some sublimation and melting/refreezing occurred in the intervening time, perhaps negatively biasing the measurements we report here. The hailstone weighed approximately 303 g. We used a 3D infrared laser scanner (e.g., Giammanco et al. 2017; Jiang et al. 2019) to obtain a high-resolution, 3D rendering of the hailstone (Fig. 9). The maximum dimension measured from the laser scan was 11.38 cm (4.48 in), which was confirmed with digital calipers (not shown).

b. Victoria's Hailstone

The most famous hailstone from the 8 February event was photographed by Victoria Druetta, a teenager living in Villa Carlos Paz. This hailstone, which we believe has the largest maximum

Accepted for publication in *Bulletin of the American Meteorological Society*. DOI 10.1175/BAMS-D-19-0012.1.

dimension documented in the Southern Hemisphere, will be referred to as "Victoria's hailstone," and it fell at the location indicated by the middle point in Fig. 1. During the RELAMPAGO field campaign, we were able to interview Victoria and her family about their experience, and obtained several additional photos and videos they took during the event.

Various photographs and video stills of Victoria's hailstone are shown in Fig. 10. Stills from a SnapChat video (Figs. 10a, b) show the hailstone shortly after it landed in the grass, taken at 4:42 pm local time (1942 UTC). Interviews with the family revealed that they watched from their living room window as the hailstone fell. "It was really impressive, we were all in shock," she recalls. She recounts that it landed near some parked cars and "smashed" when it hit the ground. Her brother told Victoria to go out and find the hailstone, telling her to wear a motorcycle helmet for safety[2]. However, she was unable to find the piece they saw break off on impact. Nonetheless, her story suggests the hailstone could have been even more massive before it was retrieved.

Figure 10c,e shows the hailstone shortly after it was retrieved from the yard. The hailstone was preserved in her freezer, and several hours later photographed again with a ruler (Fig. 10d) and weighed. At the time of the measurements (Fig. 10d), the hailstone was 18 cm in maximum dimension, to the authors' knowledge making it the largest (in terms of maximum dimension) officially documented in the Southern Hemisphere. The gargantuan hailstone weighed 442 g. There are some noticeable differences between the freshly fallen hailstone and after it had sublimated in the freezer, though we estimate the difference in maximum dimension was ≤ 1 cm between photographs. Unlike Maria's hailstone, Victoria's hailstone shows several large ($> 2-3$ cm) icicle lobes extending laterally from the particle's center of mass. These large protuberances greatly increase the maximum dimension of the particle, whereas the mass is only somewhat larger than Maria's hailstone. Further, Victoria's hailstone is only just over half the mass of the Vivian, SD

[2]Note, severe injury and/or death is still possible owing to an impact by such a large object falling at great speeds, even with a helmet. This is not recommended.

Accepted for publication in *Bulletin of the American Meteorological Society*. DOI 10.1175/BAMS-D-19-0012.1.

hailstone (which was ∼879 g), despite being within $1-2$ cm of the Vivian stone's maximum dimension. This demonstrates why cloud physicists typically are more interested in measurements of hailstone mass and volume than maximum dimension (e.g., Knight and Knight 2005).

There were at least two other extremely large hailstones that the family witnessed during this event (though did not measure or preserve). Her father recalled a stone that cracked a neighboring building's window ledge (translated from Spanish): "But that other hailstone was also something very impactful, very strong." Further, the father recounted another hailstone damaged a neighbor's vehicle (translated from Spanish):

> Here there was another vehicle parked, and a stone fell and hit between the trunk and the bumper. It made a tremendous dent. Tremendous. [The car's owner] made a claim for his car insurance because he had insurance for hail damage, but the insurance didn't want to recognize it because they requested proof. The insurance said it must have been an impact from another metal object or something like that because it couldn't have been an impact by a hailstone. We sent him proof of the television station interview that they had done with Victoria, but even then, he couldn't charge the insurance company. He had to pay for the car's damage himself.

Thus, the stone in Fig. 10 was not the only extreme hailstone to fall at the family's location during this storm.

c. Downtown Villa Carlos Paz

Finally, a high-resolution video posted on YouTube[3] features an extremely large hailstone falling in downtown Villa Carlos Paz (northernmost point in Fig. 1). During RELAMPAGO, we visited the location featured in the video and measured reference objects evident in the frame (e.g., street

[3] `https://www.youtube.com/watch?v=3Oj0WRoAi0M`; also available at `https://sites.psu.edu/kumjian/files/2019/12/GargantuanHail_VillaCarlosPaz.mp4`

light poles, widths of the green awning supports, size of sidewalk tiles, depth of the curb, etc.). We also placed rulers in the street at the estimated impact location of the hailstone, and took photographs from the estimated location and vantage point of the videographer. This allowed us to conduct the frame-by-frame photogrammetric analysis to estimate the hailstone's size. These estimates suggest the hailstone might have been a world record for maximum dimension, if officially measured. Unfortunately, the stone was not preserved or measured, precluding any official measurements.

The video shows sparse concentrations of giant hailstones falling in downtown Villa Carlos Paz, right at Paseo Central (cf. Fig. 1). There are several noteworthy impacts captured in this video, including one particularly large hailstone hitting a roofing structure (audible, but off camera), eliciting responses from onlookers and the camera operator. As the camera pans to view the impact, a few fragments are seen flying from the impact location. Then, the hailstone can be seen bouncing off an awning, falling into the street, and breaking off additional fragments as it impacts the ground. Fortunately, the initial impact with the awning slowed the hailstone and kept it more-or-less intact until it impacted the pavement, allowing it to be clearly viewed in a sequence of video frames (Fig. 11). Seconds later, another large hailstone lands on the road right next to the one at rest, explodes violently on impact, and sends shards flying several meters away.

Using the aforementioned measurements of objects in this scene, we photogrammetrically estimated the size of the hailstone from the still video frames. Of course, there are numerous sources of uncertainty and error with this type of technique, including blurred imagery in the video owing to the moving camera and/or the hailstone motion, difficulty with the image processing to distinguish the hailstone from the background, etc. The frames were carefully screened for any possible blurring from panning or hailstone motion, and ensured that enough contrast was present to separate the hailstone from the background. Six frames were found to be useful for photogrammetry

Accepted for publication in *Bulletin of the American Meteorological Society*. DOI 10.1175/BAMS-D-19-0012.1.

(Table 3). For each, we cropped out the rest of the image except for the hailstone, and transformed the color images to grayscale using color luminosity (e.g., Soderholm et al. 2020). Doing so allows for a single lightness scale. In these images, the hailstone is bright, or greater "lightness" values. For each frame, a threshold lightness value was applied to identify pixels associated with the hailstone, but not the background. The centroid of the identified hailstone pixels was then identified, as was the maximum dimension. These are shown in Figure 12. Table 3 lists the frame number, maximum dimension (in pixels), and threshold applied.

The sizes of the reference objects in the video were determined by manually counting pixels across the objects. Given that edges of objects are not sharply resolved in the video, there is a range of sizes for each object. For one extreme, we counted all pixels that deviated from the background color as part of the reference object; for the other, we only counted pixels not substantially different in color from the center or main body of the reference object. In doing so, we obtain a minimum and maximum number of pixels for a given reference object length. We took this range into consideration as a measure of uncertainty when converting the hailstone size estimates from pixels to physical units. The distribution of estimates from all 6 frames is shown in Fig. 13 and included in Table 3. Based on each of these estimates ($n = 12$), we computed the confidence interval about the mean of the hailstone maximum dimension estimates using the bias-corrected and accelerated bootstrapping technique (e.g., Efron and Tibshirani 1993) with 2000 samples. At 95% significance, the estimated maximum hail dimension is between 18.8 cm and 23.7 cm (7.4 to 9.3 inches). This would make the hailstone close to or exceeding the world record for maximum dimension, were it officially measured.

Subjectively, we assess Frames 293 and 294 to be the best estimates, based on little-to-no horizontal or blurring evident, and based on the reference objects used for the estimates (awning supports) being at the same distance from the camera as the hailstone. These two frames yield

Accepted for publication in *Bulletin of the American Meteorological Society*. DOI 10.1175/BAMS-D-19-0012.1.

maximum dimension estimates of between 22.5-28.2 cm (8.9-11.1 inches). Recall that the hailstone impacted a structure and had pieces broken off *prior* to its appearance in the video. Further, even after impacting the road (Frame 319), breaking apart further, and coming to a rest (Frame 391), our conservative estimate of the maximum dimension in the plane of view of the camera is still $\sim$15 cm (i.e., satisfies the criteria for gargantuan size). Despite the uncertainty associated with its true maximum dimension, the hailstone is impressively large.

5. Discussion and Conclusions

A new recommended category for extreme hail of sizes $>$ 15 cm in maximum dimension is proposed: "gargantuan hail." The proposed new category underscores the extreme size and damage potential of such hail, and hopefully encourages its reporting and improved documentation in other cases to better understand the storms and processes capable of producing such a hazard. This study documents such a storm, and the gargantuan hail it produced in Villa Carlos Paz, in the Córdoba province of Argentina. This case occurred over a heavily populated urban area, affording numerous eyewitnesses and social media postings. Multiple other giant hail reports were documented within city limits (not shown); thus, it was not an event with only one "freak" instance of a singular gargantuan hailstone. This indicates that gargantuan hail production can result from multiple pathways/trajectories within a storm. The video and eyewitness testimony suggests the giant and gargantuan hail was sparse in concentration and occurred at a time with little to no rain, suggesting fallout outside of the heavy precipitation core. Radar imagery supports that the gargantuan hail fell in close proximity to the updraft (as inferred from the BWER and Z_{DR} column) as it passed over Villa Carlos Paz, similar to the case analyzed in Witt et al. (2018). This is consistent with earlier arguments of size sorting offered by Browning and Foote (1976) and Browning (1977), among others.

Accepted for publication in *Bulletin of the American Meteorological Society*. DOI 10.1175/BAMS-D-19-0012.1.

The two photographed hailstones exhibited thick outer layers indicative of wet growth, consistent with other documented very large hail (Knight and Knight 2005). Wet growth can lead to icicle lobes on the hailstone surface, which can greatly increase its maximum dimension relative to its mass. Indeed, though Victoria's stone was about 58% greater in maximum dimension than Maria's stone, it was only about 28% greater in mass. Similarly, though only about 2 cm smaller in maximum dimension than the Vivian, SD record hailstone, its mass was only about half (50.3%) of the Vivian hailstone's mass. This underscores the need to better characterize hailstones by *mass*, in addition to maximum dimension.

Unsurprisingly, the storm that produced the gargantuan hail in Villa Carlos Paz was a supercell, consistent with studies by Blair et al. (2011) and Blair et al. (2017) and earlier studies suggesting supercells are capable of large hail (e.g., Nelson 1983; Foote 1984; Rasmussen and Heymsfield 1987; Miller et al. 1990; Tessendorf et al. 2005). Aside from being broadly conducive for supercells and thus hail production, nothing in the environment indicated conditions favorable for such extreme hail production. Further, the storm's radar presentation as observed with the operational C-band RMA1 radar was not atypical of supercells. The 1-km grid spacing WRF simulation of this case, despite closely following the observed storm evolution, also did not indicate anything out of the ordinary for supercellular convection, though it did highlight the rapid environmental evolution leading up to the storm.

The lack of indications of an extreme event in the pre-storm environment, numerical model forecasts, or radar imagery collectively demonstrate the challenges associated with forecasting or even detecting extreme hail events. Further research is needed to better understand the environmental conditions leading to storms capable of producing gargantuan hail, radar signatures of gargantuan hail, and the climatology of such events. We encourage local forecast offices, broadcast meteorologists, and emergency managers to interface with and educate the public during severe convective

Accepted for publication in *Bulletin of the American Meteorological Society*. DOI 10.1175/BAMS-D-19-0012.1.

storm episodes to better document the occurrence of gargantuan hail, including accurate time and location of hail fall, and accurate measurements of hailstone size, especially mass. Such documentation will facilitate an improved understanding of the storms capable of producing such hazardous hail.

Acknowledgments. We would like to thank the National Science Foundation Grants AGS-1661679 and AGS-1855063, and an award from the Insurance Institute for Business and Home Safety (IBHS). We thank IBHS for lending us their 3D laser scanner, and particularly Ross Maiden for training the lead author on its use. ERA5 data are from the European Centre for Medium-Range Weather Forecasting (ECMWF), acquired through the Copernicus Climate Change Service Climate Data Store (CDS). RMA1 data were provided by Secretaría de Infraestructura y Política Hídrica, Ministerio del Interior, Obras Públicas y Vivienda of the Argentinean National Government within the SINARAME Project. The National System of Weather Radars (Sistema Nacional de Radares Meteorológicos, SINARAME) project is an Argentinean effort to expand the radar network over the nation. We also thank the citizens of Villa Carlos Paz for their time and accommodation during RELAMPAGO. In particular, we are very grateful to Victoria Druetta and her family, and to Maria Navidad Garay. Finally, we thank the 3 anonymous reviewers for their criticisms and constructive comments on the manuscript, which helped produce a substantially improved manuscript.

References

Blair, S. F., D. Deroche, J. M. Boustead, J. W. Leighton, B. L. Barjenbruch, and G. W. P, 2011: A radar-based assesment of the detectability of giant hail. *Electr. J. Severe Storms Meteor.*, **6(7)**, 1–30.

Accepted for publication in *Bulletin of the American Meteorological Society*. DOI 10.1175/BAMS-D-19-0012.1.

Blair, S. F., and J. W. Leighton, 2012: Creating high-resolution hail datasets using social media and post-storm ground surveys. *Electr. J. Oper. Meteor.*, **13(3)**, 32–45.

Blair, S. F., and Coauthors, 2017: High-resolution hail observations: implications for NWS warning operations. *Wea. Forecasting*, **32**, 1101–1119.

Browning, K. A., 1977: The structure and mechanisms of hailstorms. *"Meteor. Monogr."*, **38**, 1–43.

Browning, K. A., and R. J. Donaldson, 1964: Airflow and structure of a tornadic storm. *J. Atmos. Sci.*, **20**, 533–545.

Browning, K. A., and G. B. Foote, 1976: Air-flow and hail growth in supercell storms and some implications for hail suppression. *Quart. J. Roy. Meteor. Soc.*, **102**, 499–533.

Bruick, Z. S., K. L. Rasmussen, and D. J. Cecil, 2019: Subtropical South American hailstorm characteristics and environments. *Mon. Wea. Rev.*, **147**, 4289–4304.

Bunkers, M. J., B. A. Klimowski, J. W. Zeitler, R. L. Thompson, and M. L. Weisman, 2000: Predicting supercell motion using a new hodograph technique. *Weather and Forecasting*, **15**, 61–79.

Cecil, D. J., and C. B. Blankenship, 2012: Toward a global climatology of severe hailstorms as estimated by satellite passive microwave imagers. *J. Climate*, **25**, 687–703.

Coffer, B. E., and M. D. Parker, 2017: Simulated supercells in nontornadic and tornadic VORTEX2 environments. *Mon. Wea. Rev.*, **145**, 149–180.

Copernicus Climate Change Service, 2019: ERA5: Fifth generation of ECMWF atmospheric reanalyses of the global climate. Copernicus Climate Change Service Climate Data Store, accessed 12 April 2019. [Available online at https://cds.climate.copernicus.eu/cdsapp#!/home.].

Dennis, E. J., and M. R. Kumjian, 2017: The impact of vertical wind shear on hail growth in simulated supercells. *J. Atmos. Sci.*, **74**, 641–663.

Efron, B., and R. J. Tibshirani, 1993: An introduction to the bootstrap. Chapman and Hall, 456 pp.

Foote, G. B., 1984: A study of hail growth utilizing observed storm conditions. *J. Climate Appl. Meteor.*, **23**, 84–101.

Giammanco, I. M., B. R. Maiden, H. E. Estes, and T. M. Brown-Giammanco, 2017: Using 3D laser scanning technology to create digital models of hailstones. *Bull. Amer. Meteor. Soc.*, **98**, 1341–1347.

Gutierrez, R., 2019: Environmental and radar characteristics of gargantuan-hail-producing storms. M.S. thesis, Dept. of Meteorology and Atmospheric Science, The Pennsylvania State University, 68 pp., available from The Pennsylvania State University Electronic Thesis and Dissertation database.

Hubbert, J. C., and V. N. Bringi, 2000: The effects of three-body scattering on differential reflectivity signatures. *J. Atmos. Oceanic Technol.*, **17**, 51–61.

Jiang, Z., M. R. Kumjian, R. S. Schrom, I. Giammanco, T. Brown-Giammanco, H. Estes, R. Maiden, and A. J. Heymsfield, 2019: Comparisons of electromagnetic scattering properties of real hailstones and spheroids. *J. Appl. Meteor. Climatol.*, **58**, 93–112.

Knight, C. A., and N. C. Knight, 1970: Lobe structures of hailstones. *J. Atmos. Sci.*, **27**, 667–671.

Knight, C. A., and N. C. Knight, 2001: Hailstorms. *Meteor. Monogr.*, **50**, 223–248.

Knight, C. A., and N. C. Knight, 2005: Very large hailstones from Aurora, Nebraska. *Bull. Amer. Meteor. Soc.*, **86**, 1773–1781.

Accepted for publication in *Bulletin of the American Meteorological Society*. DOI 10.1175/BAMS-D-19-0012.1.

Kumjian, M., J. Picca, S. Ganson, A. V. Ryzhkov, J. Krause, and A. P. Khain, 2010: Polarimetric radar characteristics of large hail. Extended Abstracts, *25th Conf. on Severe Local Storms*, Denver, CO, Amer. Meteor. Soc., 11.2, [Available online at https://ams.confex.com/ams/pdfpapers/176043.pdf].

Kumjian, M. R., 2013a: Principles and applications of dual-polarization weather radar. part II: Warm and cold season applications. *J. Operational Meteor.*, **1**, 243–264, doi:10.15191/nwajom.2013.0120.

Kumjian, M. R., 2013b: Principles and applications of dual-polarization weather radar. part III: Artifacts. *J. Operational Meteor.*, **1**, 265–274, doi:10.15191/nwajom.2013.0121.

Kumjian, M. R., 2018: Weather radars. *Remote Sensing of Clouds and Precipitation*, C. Andronache, Ed., Springer, 15–63.

Kumjian, M. R., A. P. Khain, N. BenMoshe, E. Ilotoviz, A. V. Ryzhkov, and V. T. J. Phillips, 2014: The anatomy and physics of Z_{DR} columns: Investigating a polarimetric radar signature with a spectral bin microphysical model. *J. Appl. Meteor. Climatol.*, **53**, 1820–1843.

Kumjian, M. R., and A. V. Ryzhkov, 2008: Polarimetric signatures in supercell thunderstorms. *J. Appl. Meteor. Climatol.*, **47**, 1940–1967.

Markowski, P. M., 2002: Hook echoes and rear-flank downdrafts: A review. *Mon. Wea. Rev.*, **130**, 852–876.

Markowski, P. M., and Y. P. Richardson, 2014: The influence of environmental low-level shear and cold pools on tornadogenesis: Insights from idealized simulations. *J. Atmos. Sci.*, **71**, 243–275.

Marwitz, J. D., 1972: The structure and motion of severe hailstorms. Part I: Supercell storms. *J. Appl. Meteor.*, **11**, 166–179.

Accepted for publication in *Bulletin of the American Meteorological Society*. DOI 10.1175/BAMS-D-19-0012.1.

Mezher, R. N., M. Doyle, and V. Barros, 2012: Climatology of hail in Argentina. *Atmos. Res.*, **114-115**, 70–82.

Miller, L. J., J. D. Tuttle, and G. B. Foote, 1990: Precipitation production in a large Montana hailstorm - Air-flow and particle growth trajectories. *J. Atmos. Sci.*, **47**, 1619–1646.

Mulholland, J. P., S. W. Nesbitt, and R. J. Trapp, 2019: A case study of terrain influences on upscale convective growth of a supercell. *Mon. Wea. Rev.*, **147**, 4305–4324.

Mulholland, J. P., S. W. Nesbitt, R. J. Trapp, K. L. Rasmussen, and P. V. Salio, 2018: Convective storm life cycle and environments near the Sierras de Córdoba, Argentina. *Mon. Wea. Rev.*, **146 (8)**, 2541–2557.

Nelson, S. P., 1983: The influence of storm flow structure on hail growth. *J. Atmos. Sci.*, **40**, 1965–1983.

Picca, J. C., and A. V. Ryzhkov, 2012: A dual-wavelength polarimetric analysis of the 16 May 2010 Oklahoma City extreme hailstorm. *Mon. Wea. Rev.*, **140**, 1385–1403.

Pojorlie, K. L., S. Doering, and M. A. Fowle, 2013: The record-breaking Vivian, South Dakota hailstorm of 23 July 2010. *J. Oper. Meteor.*, **1(2)**, 3–18.

Rasmussen, R. M., and A. J. Heymsfield, 1987: Melting and shedding of graupel and hail. Part III: Iinvestigation of the role of shed drops as hail embryos in the 1 August CCOPE severe storm. *J. Atmos. Sci.*, **44**, 2783–2803.

Ryzhkov, A. V., M. R. Kumjian, S. M. Ganson, and A. P. Khain, 2013: Polarimetric radar characteristics of melting hail. Part 1: Theoretical simulations using spectral microphysical modeling. *J. Appl. Meteor. Climatol.*, **52**, 2849–2870.

Accepted for publication in *Bulletin of the American Meteorological Society*. DOI 10.1175/BAMS-D-19-0012.1.

Seimon, A., J. T. Allen, T. A. Seimon, S. Talbot, and D. K. Hoadley, 2016: Crowdsourcing the El Reno 2013 tornado: A new approach for collation and display of storm chaser imagery for scientific applications. *Bull. Amer. Meteor. Soc.*, **97**, 2069–2084.

Skamarock, W. C., J. B. Klemp, J. Dudhia, D. O. Gill, D. M. Barker, W. Wang, and J. G. Powers, 2008: A description of the advanced research wrf version 3. *NCAR Technical Note*.

Soderholm, J., M. Kumjian, N. McCarthy, P. Maldonado, and M. Wang, 2020: Quantifying hail size distributions from the sky: Application of drone aerial photogrammetry. *Atmos. Meas. Tech. Disc.*, **conditionally accepted**.

Tessendorf, S. A., L. J. Miller, K. C. Wiens, and S. A. Rutledge, 2005: The 29 June supercell observed during STEPS. Part I: Kinematics and microphysics. *J. Atmos. Sci.*, **62**, 4127–4150.

Thompson, G., R. M. Rasmussen, and K. Manning, 2004: Explicit forecasts of winter precipitation using an improved bulk microphysics scheme. part i: Description and sensitivity analysis. *Monthly Weather Review*, **132 (2)**, 519–542, doi:10.1175/1520-0493(2004)132⟨0519:EFOWPU⟩2.0.CO;2, URL https://doi.org/10.1175/1520-0493(2004)132⟨0519:EFOWPU⟩2.0.CO;2, https://doi.org/10.1175/1520-0493(2004)132⟨0519:EFOWPU⟩2.0.CO;2.

Torre, A. D. L., R. Hierro, P. Llamedo, A. Rolla, and P. Alexander, 2011: Severe hailstorms near the Southern Andes in the presence of mountain waves. *Atmos. Res.*, **101**, 112–123.

Warren, R. A., H. Richter, H. A. Ramsay, S. T. Siems, and M. J. Manton, 2017: Impact of variations in upper-level shear on simulated supercells. *Mon. Wea. Rev.*, **145**, 2659–2681.

Witt, A., D. W. Burgess, A. Seimon, J. T. Allen, J. C. Snyder, and H. B. Bluestein, 2018: Rapid-scan radar observations of an Oklahoma tornadic hailstorm producing giant hail. *Wea. Forecasting*, **33**, 1263–1282.

Accepted for publication in *Bulletin of the American Meteorological Society*. DOI 10.1175/BAMS-D-19-0012.1.

Zrnić, D. S., G. Zhang, V. Melnikov, and J. Andrić, 2010: Three-body scattering and hail size. *J. Appl. Meteor. Climatol.*, **49**, 687–700.

Accepted for publication in *Bulletin of the American Meteorological Society*. DOI 10.1175/BAMS-D-19-0012.1.

LIST OF TABLES

Accepted for publication in *Bulletin of the American Meteorological Society*. DOI 10.1175/BAMS-D-19-0012.1.

TABLE 1: Proposed hail size naming convention, based on previous usage and operational terminology.

Size Class	Maximum Dimension Threshold (cm)	Reference Object	References
Small / Sub-Severe	≤ 2.5	$\leq$ U.S. quarter coin	NWS; Ryzhkov et al. (2013)
Severe	≥ 2.5	$\geq$ U.S. quarter coin	NWS
Significantly Severe	≥ 5.0	$\geq$ hen egg	NWS
Giant	≥ 10.0	$\geq$ softball	Knight and Knight (2005), Blair et al. (2011)
Gargantuan	≥ 15.0	$\geq$ honeydew melon	Proposed in this study, Gutierrez (2019)

Accepted for publication in *Bulletin of the American Meteorological Society*. DOI 10.1175/BAMS-D-19-0012.1.

TABLE 2: Maximum dimension, mass, and location of the three large hailstones documented in this study.

Hailstone	Maximum Dimension (cm)	Mass (g)	Latitude, Longitude
Maria's hailstone	11.38	303	-31.426521°, -64.495426°
Victoria's hailstone	18.00	422	-31.424431°, -64.497983°
Paseo Central (Video)	18.8-23.7	unknown	-31.420750°, -64.499738°

Accepted for publication in *Bulletin of the American Meteorological Society*. DOI 10.1175/BAMS-D-19-0012.1.

TABLE 3: Frames used for the photogrammetric analysis, from Fig. 12. Maximum dimension of the hailstone in the image (in pixels) is given, as is the threshold used by the image processing routine, and the minimum and maximum size estimate (in cm). The asterisk indicates the frame is from when the camera was zoomed in on the hailstone.

Frame	Maximum Dimension (pixels)	Threshold Used (%)	Maximum Dimension Range (cm)
293	25.02	45	23.9 – 28.2
294	23.54	50	22.5 – 26.6
316	25.32	45	20.4 – 24.8
317	23.09	61	18.6 – 22.6
319	17.69	69	14.2 – 17.3
391*	21.84	93	14.7 – 21.1

Accepted for publication in *Bulletin of the American Meteorological Society*. DOI 10.1175/BAMS-D-19-0012.1.

LIST OF FIGURES

Accepted for publication in *Bulletin of the American Meteorological Society*. DOI 10.1175/BAMS-D-19-0012.1.

Accepted for publication in *Bulletin of the American Meteorological Society*. DOI 10.1175/BAMS-D-19-0012.1.

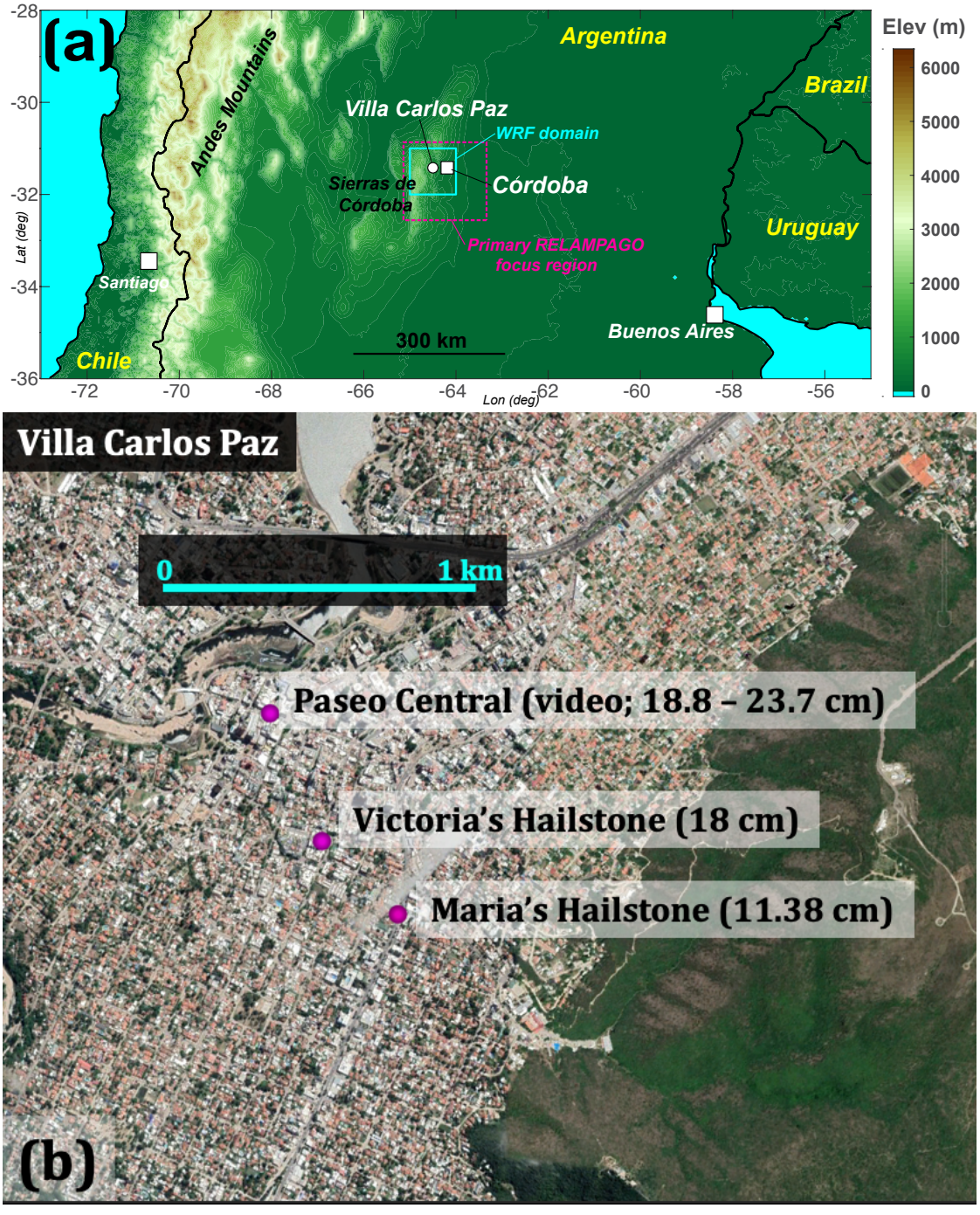

FIG. 1: (a) Map of the region of interest in South America, including WRF simulation innermost domain (cyan box) and the approximate RELAMPAGO study region (light purple dashed box). The locations of Córdoba and Villa Carlos Paz are indicated as white square and circle markers, respectively. The map shows terrain elevation, shaded according to the outset scale on the right. Black solid lines are country boundaries. (b) Zoom into downtown Villa Carlos Paz, Argentina, and the location of 3 hailstones analyzed herein (with maximum dimensions indicated, in cm). Map imagery courtesy of Google.

Accepted for publication in *Bulletin of the American Meteorological Society*. DOI 10.1175/BAMS-D-19-0012.1.

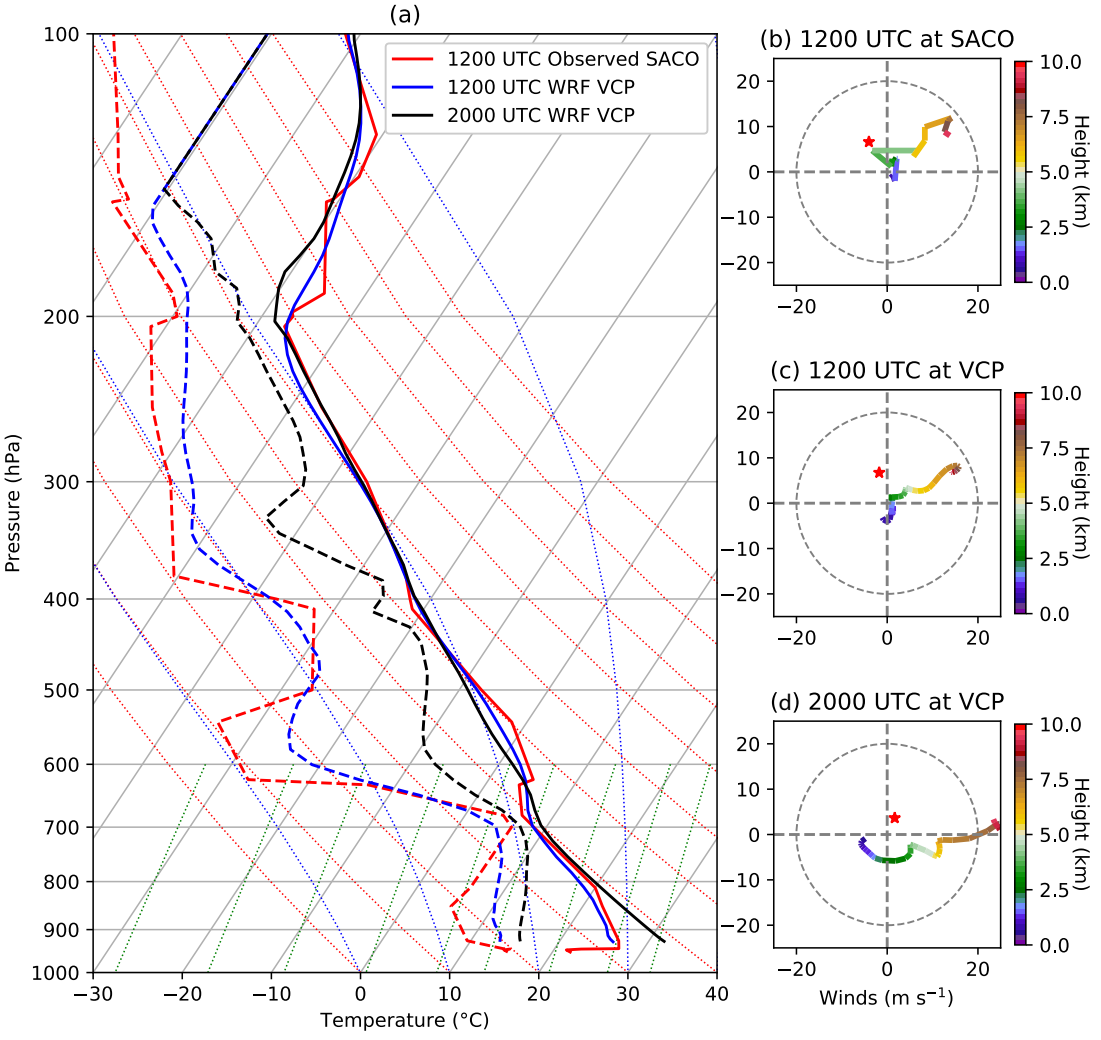

FIG. 2: (a) Thermodynamic soundings at SACO (observed at 12 UTC, in red) and VCP (simulated at 12 and 20 UTC, in blue and black, respectively), with temperature given by the solid line and dewpoint temperature given by the dashed line. (b) 12 UTC SACO observed 0-10−km hodograph, with the Bunkers et al. (2000) left-moving supercell motion shown by the red star. Panels (c) and (d) are as in (b), but simulated at VCP at 12 and 20 UTC.

Accepted for publication in *Bulletin of the American Meteorological Society*. DOI 10.1175/BAMS-D-19-0012.1.

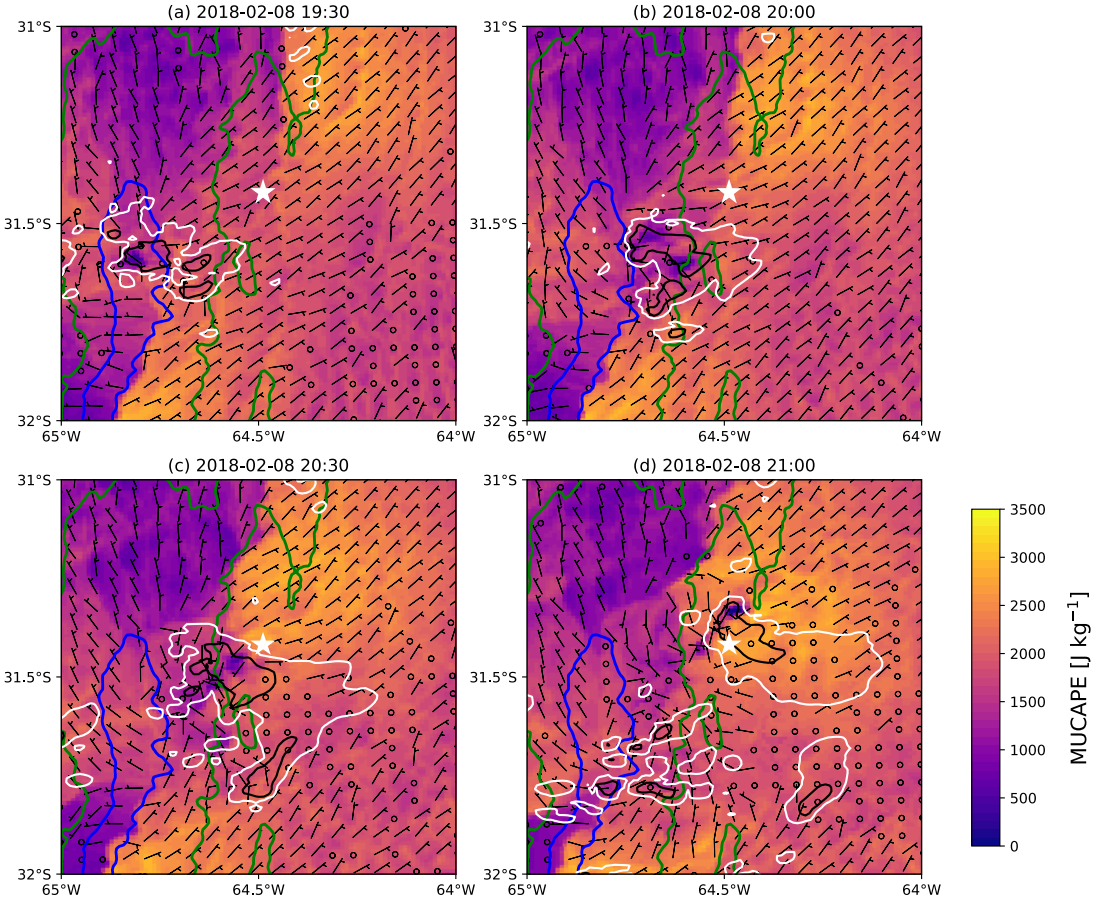

FIG. 3: Output of the WRF simulation of this event, shown at (1) 19:30, (b) 20:00, (c) 20:30, and (d) 21:00 UTC. Shaded are values of MUCAPE (J kg^{-1}, with colorbar at lower right), contour values are selected values of simulated Z_H (20 and 40 dBz in white and black contours, respectively). Terrain at 1000 and 2000 m is shown with the green and blue contours, respectively. 10-m wind barbs are shown (full barb = 10 m s^{-1}). The white star shows the location of Villa Carlos Paz.

Accepted for publication in *Bulletin of the American Meteorological Society*. DOI 10.1175/BAMS-D-19-0012.1.

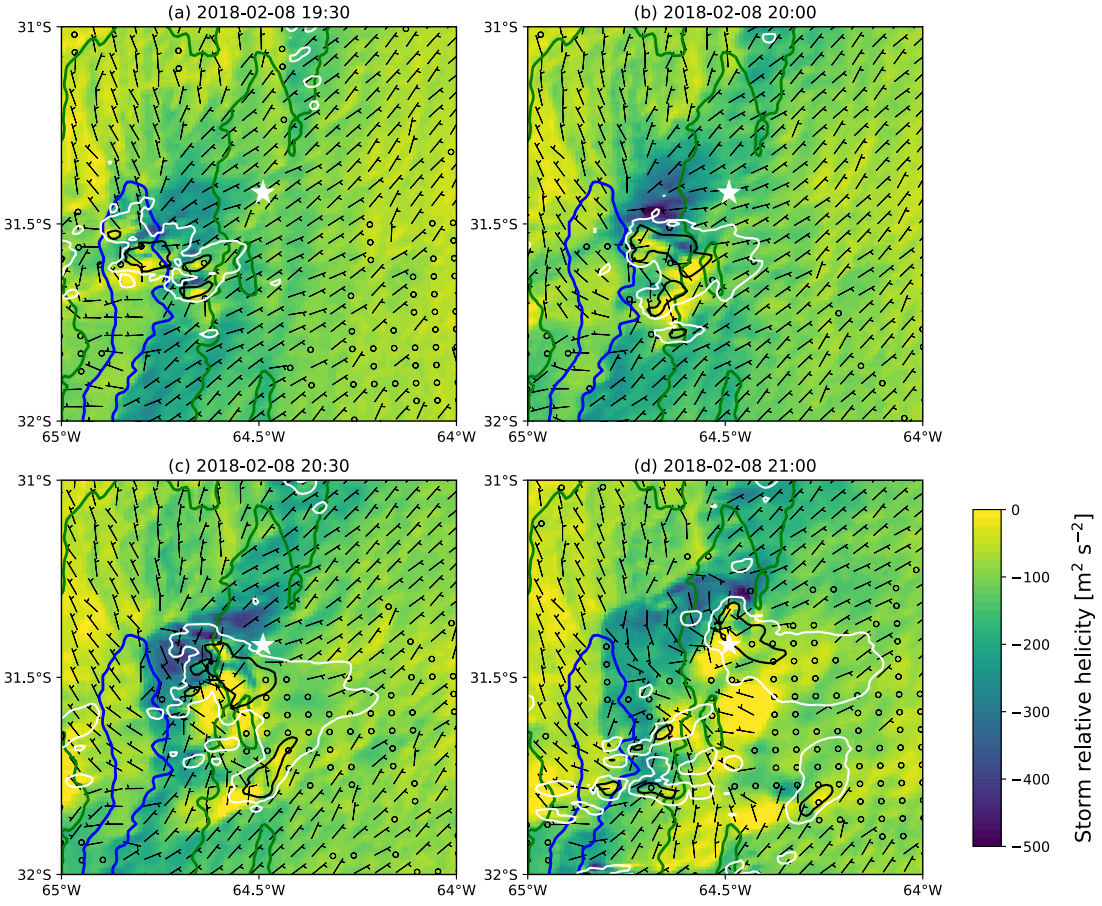

FIG. 4: As in Fig. 3, except 0-3 km storm-relative helicity (SRH; m^2 s^{-2}) is shaded.

Accepted for publication in *Bulletin of the American Meteorological Society*. DOI 10.1175/BAMS-D-19-0012.1.

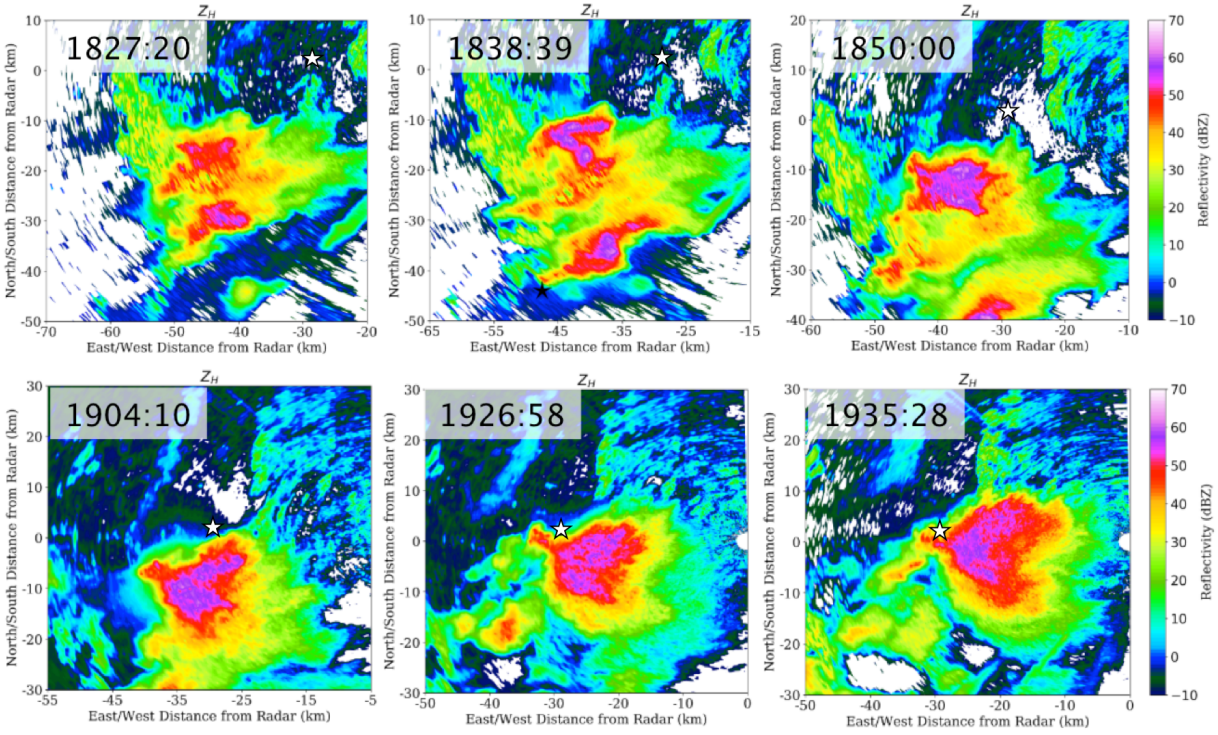

FIG. 5: Evolution of the storm as depicted by low-level Z_H scans (shaded in dBz, according to the scale) from the RMA1 radar. The white star shows the location of Villa Carlos Paz in each panel. Elevation angles shown are 1.54°, 1.49°, 1.58°, 1.85°, 1.80°, 1.49°.

Accepted for publication in *Bulletin of the American Meteorological Society*. DOI 10.1175/BAMS-D-19-0012.1.

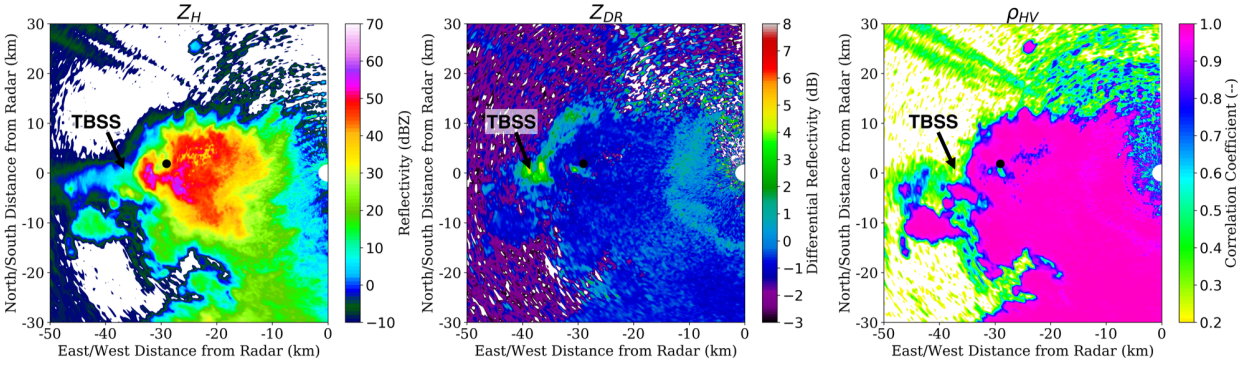

FIG. 6: A selected PPI scan from 11° elevation angle, taken at 1926:58 UTC, around the time the storm was producing gargantuan hail. Panels shown are (a) Z_H, (b) Z_{DR}, (c) ρ_{hv}. The annotated arrow indicates the polarimetric three-body scattering signature. The black dot is Villa Carlos Paz.

Accepted for publication in *Bulletin of the American Meteorological Society*. DOI 10.1175/BAMS-D-19-0012.1.

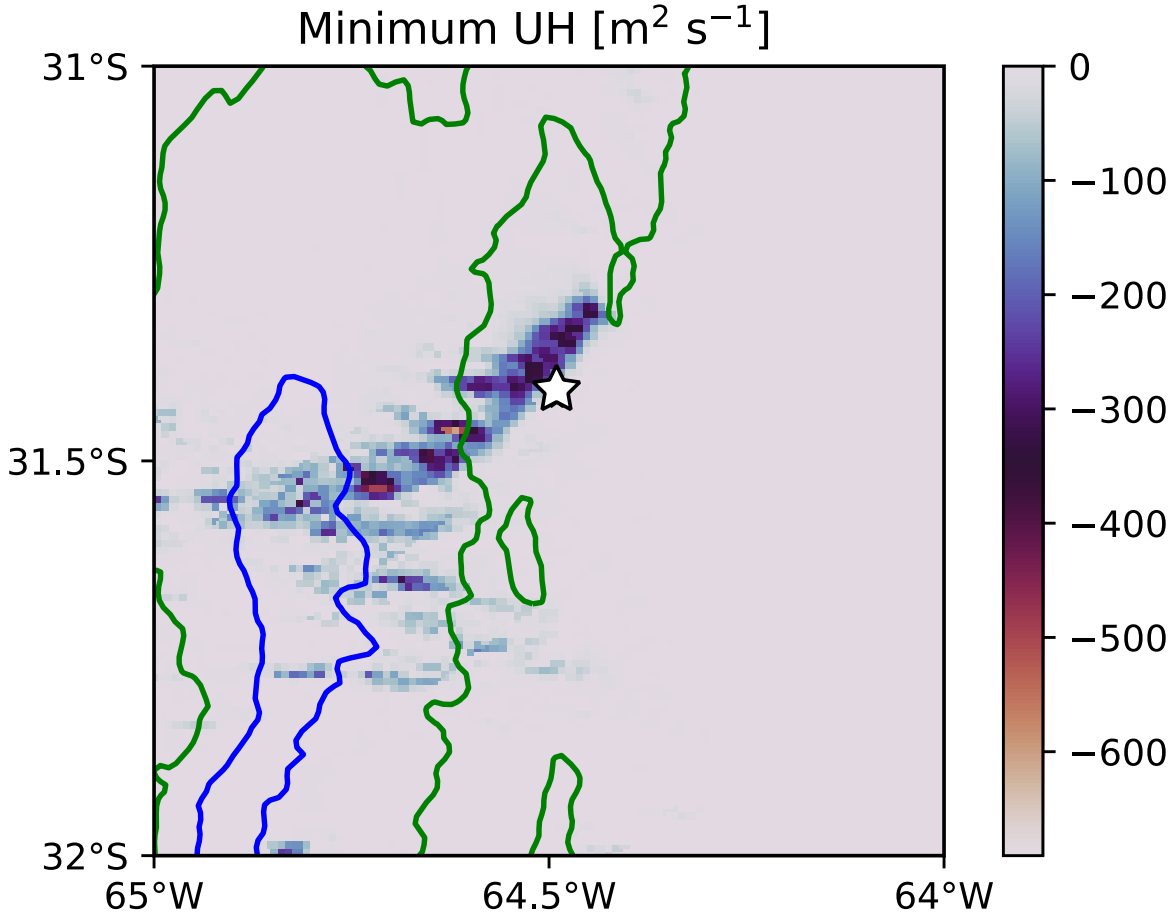

FIG. 7: Plan views of WRF simulated minimum updraft helicity (UH; m^2 s^{-1}). Green and blue contours show the terrain at 1000 and 2000 m, respectively, and the white star shows the location of Villa Carlos Paz.

Accepted for publication in *Bulletin of the American Meteorological Society*. DOI 10.1175/BAMS-D-19-0012.1.

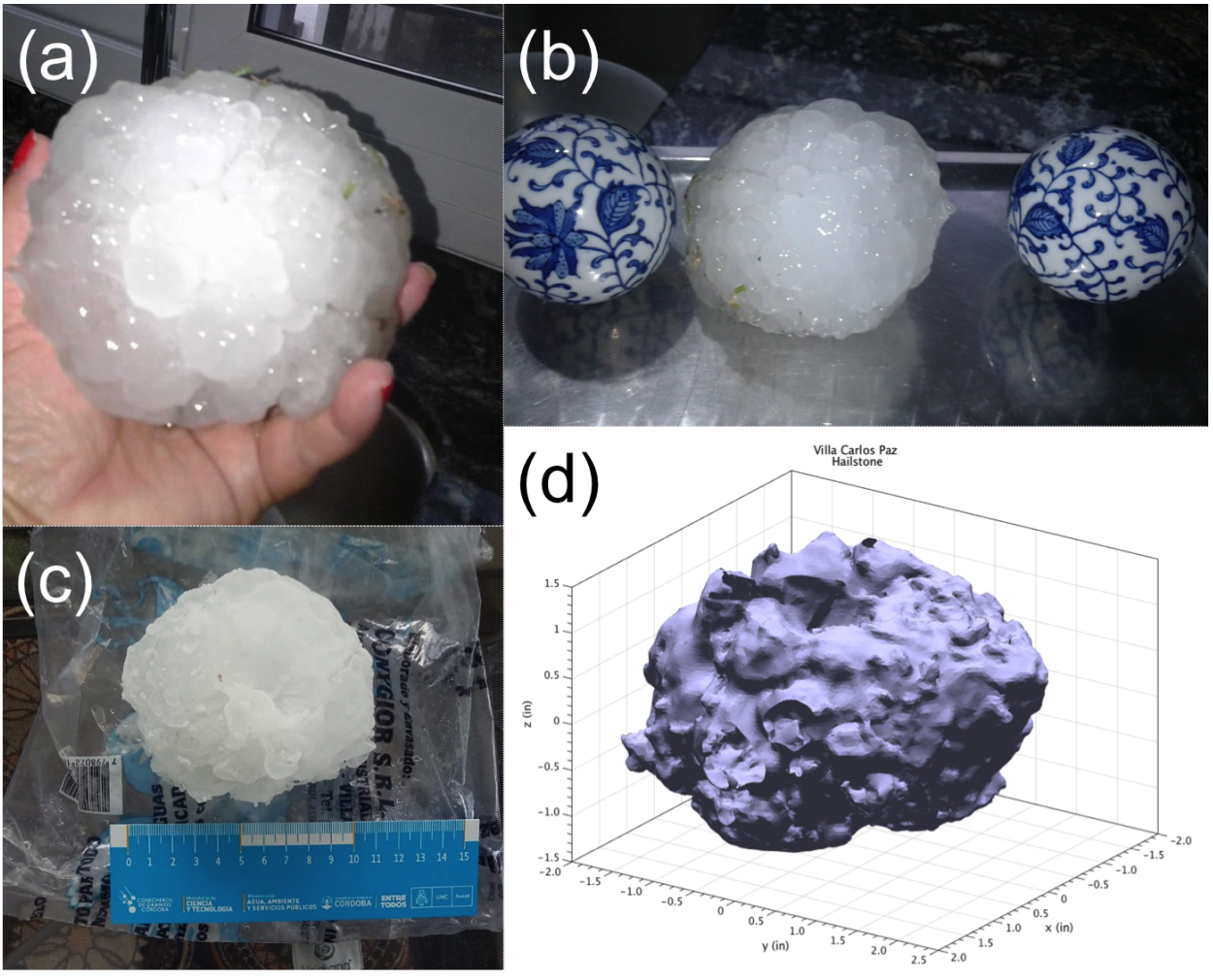

FIG. 8: (a) Photograph of Maria's hailstone shortly after it was retrieved from her front yard. (b) Photograph of the giant hailstone next to decorative balls, which measured 7.5 cm in diameter (as measured with digital calipers, not shown). Photos courtesy of Maria Navidad Garay, used with permission. (c) Photograph of preserved hailstone after being in the freezer for 9 months, with ruler for comparison. (d) 3D rendering of the laser-scanned hailstone.

Accepted for publication in *Bulletin of the American Meteorological Society*. DOI 10.1175/BAMS-D-19-0012.1.

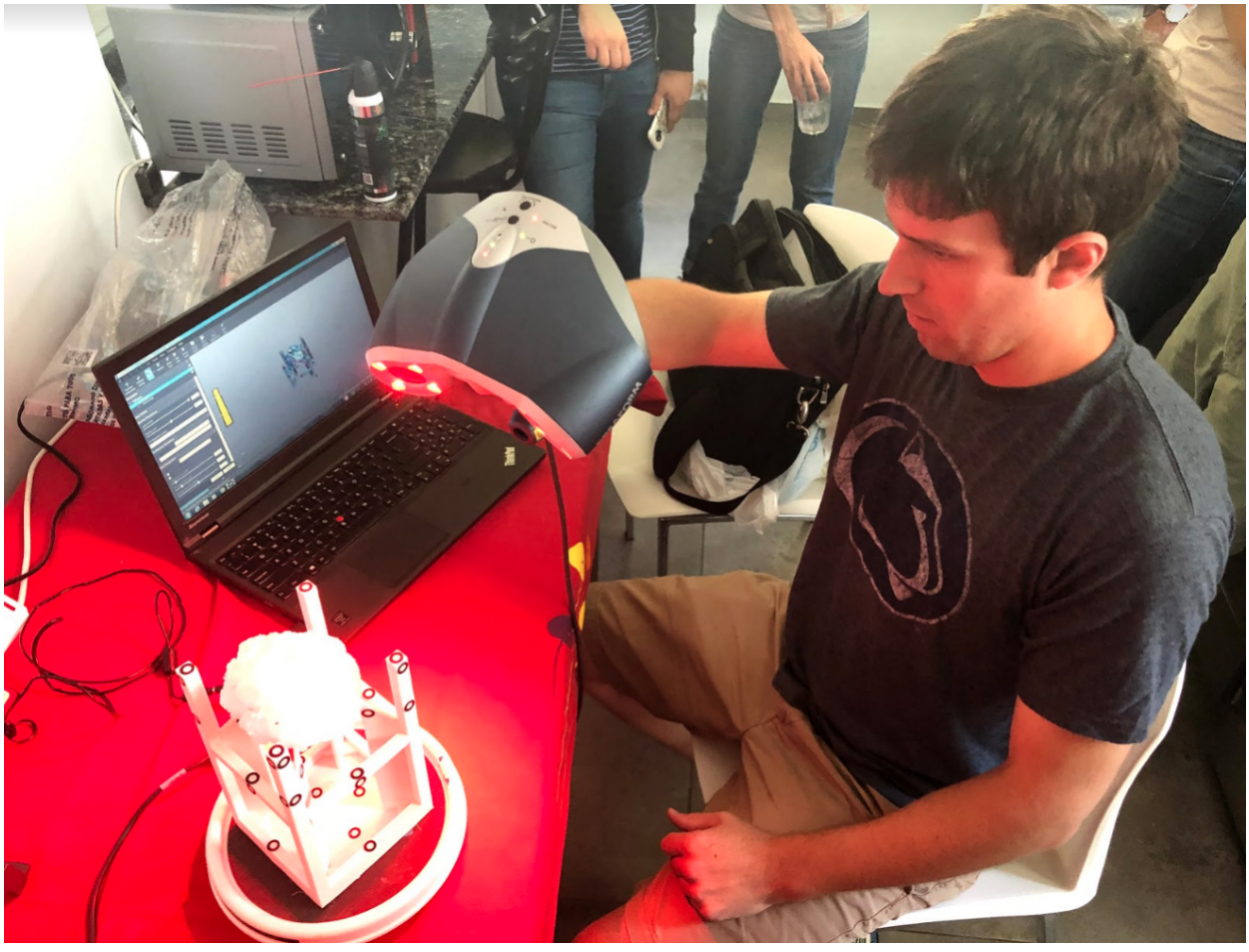

FIG. 9: Photograph of Maria's hailstone being scanned using the 3D laser scanner, which affords high-resolution maps of the hailstone's detailed shape. Photograph courtesy of J. Marquis, used with permission

Accepted for publication in *Bulletin of the American Meteorological Society*. DOI 10.1175/BAMS-D-19-0012.1.

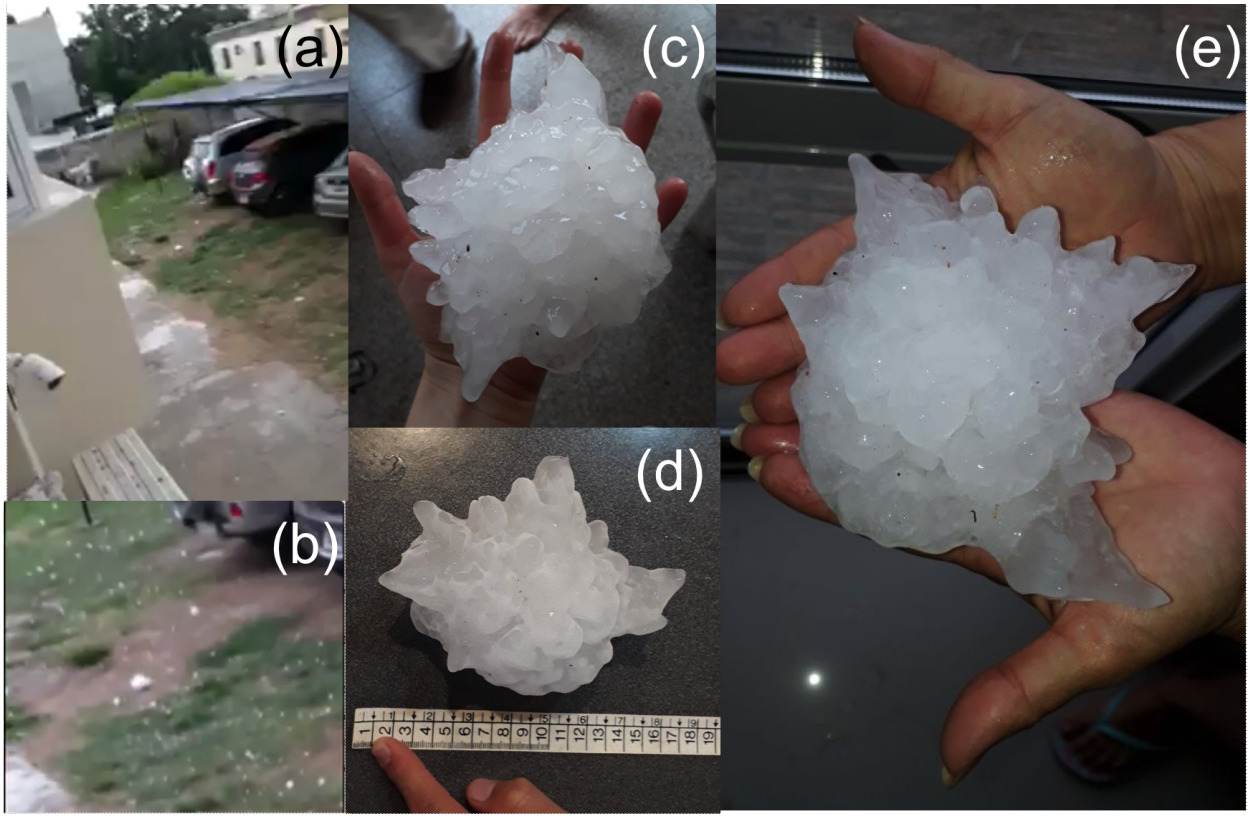

FIG. 10: (a), (b) Screenshots of a Snapchat video of Victoria's hailstone shortly after it landed. (c) Photograph of the hailstone in hand just after retrieving it. (d) Official measurement, after noticeable sublimation and melting: 18 cm (7.1 in) in maximum dimension, 422 g in mass. (e) Viral photo of her mother holding the stone, shortly after it was retrieved. Photogrammetry based on measurements of their hands suggests the maximum size after it was retrieved is close to 19 cm. All imagery provided courtesy of Victoria Druetta, used with permission.

Accepted for publication in *Bulletin of the American Meteorological Society*. DOI 10.1175/BAMS-D-19-0012.1.

FIG. 11: Sequence of frames from a YouTube video taken in downtown Villa Carlos Paz, showing a gargantuan hailstone (annotated with blue arrows in each panel). The frame numbers from the video are included in each panel.

Accepted for publication in *Bulletin of the American Meteorological Society*. DOI 10.1175/BAMS-D-19-0012.1.

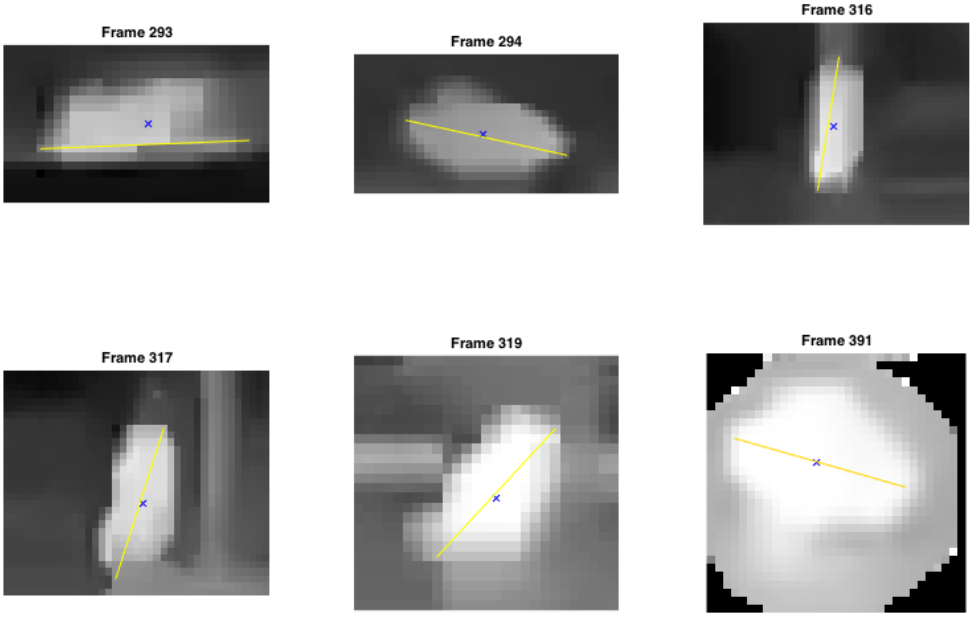

FIG. 12: Grayscale images of the gargantuan hailstone extracted from the YouTube video. The blue "X" marker indicates the hailstone centroid, and the yellow line shows the maximum dimension determined by the image processing. The final image (Frame 391) has been manually cropped to eliminate other hail fragments on the road.

Accepted for publication in *Bulletin of the American Meteorological Society*. DOI 10.1175/BAMS-D-19-0012.1.

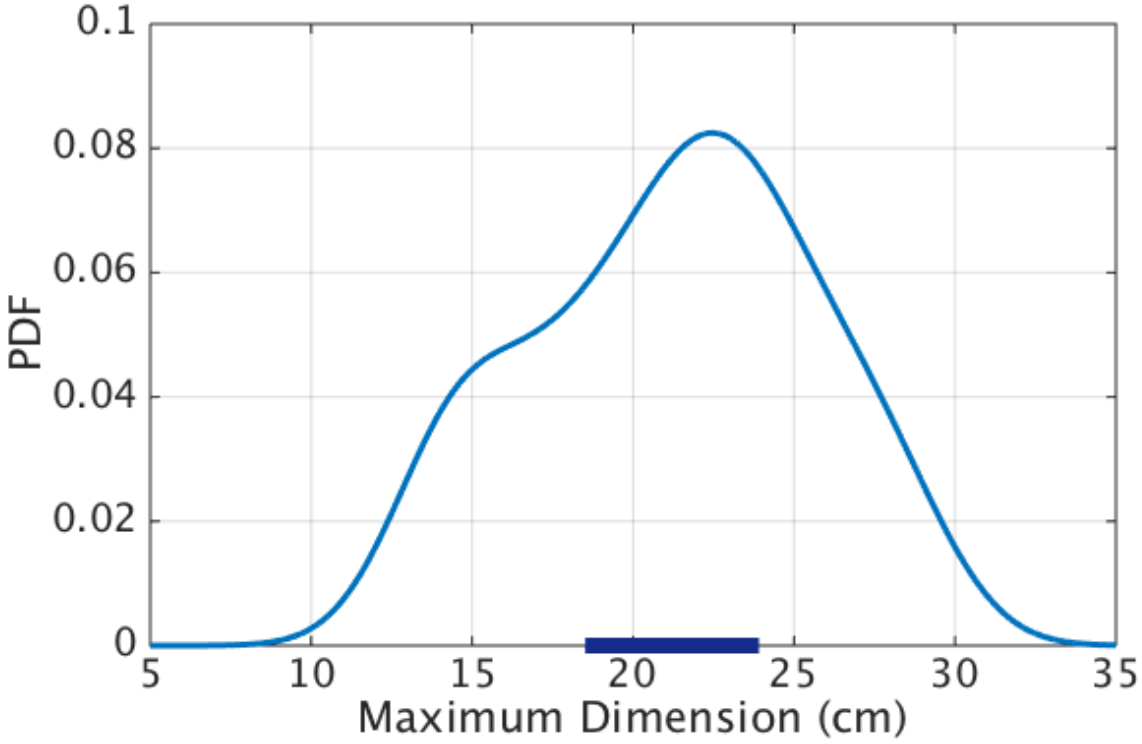

FIG. 13: Kernel density estimate (bandwidth = 2 cm) of the distribution of maximum dimension estimates (cm) from the photogrammetric analyses. Overlaid are the confidence intervals about the mean of estimates at 95% significance (bar along abscissa).

Accepted for publication in *Bulletin of the American Meteorological Society*. DOI 10.1175/BAMS-D-19-0012.1.